Available online at www.sciencedirect.com
SCIENCE DIRECT®
Nuclear Instruments and Methods in Physics Research A 514 (2003) 47–61
NUCLEAR INSTRUMENTS & METHODS IN PHYSICS RESEARCH Section A
www.elsevier.com/locate/nima

The effect of charge collection recovery in silicon p–n junction detectors irradiated by different particles ☆

E. Verbitskaya[a,*], M. Abreu[b], P. Anbinderis[c], T. Anbinderis[c], N. D'Ambrosio[d], W. de Boer[e], E. Borchi[f], K. Borer[g], M. Bruzzi[f], S. Buontempo[d], L. Casagrande[h], W. Chen[i], V. Cindro[j], B. Dezillie[i], A. Dierlamm[e], V. Eremin[a], E. Gaubas[c], V. Gorbatenko[c], V. Granata[k,1], E. Grigoriev[e,l,2], S. Grohmann[h], F. Hauler[e], E. Heijne[h], S. Heising[e], O. Hempel[m], R. Herzog[m], J. Härkönen[n], I. Ilyashenko[a], S. Janos[g], L. Jungermann[e], V. Kalesinskas[c], J. Kapturauskas[c], R. Laiho[o], Z. Li[i], I. Mandic[j], Rita De Masi[p], D. Menichelli[f], M. Mikuz[j], O. Militaru[q], T.O. Niinikoski[h], V. O'Shea[r], S. Pagano[d], V.G. Palmieri[h], S. Paul[p], B. Perea Solano[h], K. Piotrzkowski[q], S. Pirollo[f], K. Pretzl[g], P. Rato Mendes[b], G. Ruggiero[r], K. Smith[r], P. Sonderegger[h], P. Sousa[b], E. Tuominen[n], J. Vaitkus[c], C. da Viá[k], E. Wobst[m], M. Zavrtanik[j]

[a] *Ioffe Physico-Technical Institute, Russian Academy of Sciences, St. Petersburg 194021, Russia*
[b] *LIP, Av. E. Garcia, Lisbon P-1000, Portugal*
[c] *University of Vilnius, Institute of Materials Science and Applied Research, Vilnius 2040, Lithuania*
[d] *Dipartimento di Fisica, Universitá "Federico II" and INFN, Napoli I-80125, Italy*
[e] *IEKP University of Karlsruhe, Karlsruhe D-76128, Germany*
[f] *Dipartimento di Energetica, Universitá di Firenze, Firenze I-50139, Italy*
[g] *Laboratorium für Hochenergiephysik der Universität Bern, Sidlerstarsse 5, Bern CH-3012, Switzerland*
[h] *CERN, Geneva CH-1211, Switzerland*
[i] *Brookhaven National Laboratory, Upton, NY 11973-5000, USA*
[j] *Jozef Stefan Institute, Exp. Particle Physics Dep., P.O. Box 3000, Ljubljana 1001, Slovenia*
[k] *Brunel University, Uxbridge, Middlesex UB8 3PH, UK*
[l] *Department de Radiologie, Universite de Geneve, Geneva CH-1211, Switzerland*
[m] *ILK Dresden, Bertolt-Brecht-Allee 20, Dresden 01309, Germany*
[n] *Helsinki Institute of Physics, P.O.Box 64, University of Helsinki 00014, Finland*
[o] *University of Turku, Wihuri Physical Laboratory, Turku FI-20014, Finland*
[p] *Physik Department E18, Technische Universität München, Garching D-85748, Germany*
[q] *Université Catholique de Louvain, Louvain-la-Neuve B-1348, Belgium*
[r] *Department of Physics and Astronomy, University of Glasgow, Glasgow G12 8QQ, UK*

RD39 Collaboration

☆ This work has been supported in part by INTAS-CERN: project no. 993-850, Russian Foundation for Basic Research: Grant no. 00-15-96750, and U.S. Department of Energy: Contract No. DE-Ac02-98CH10886.

*Corresponding author. Tel.: +7-812-247-9953; fax: +7-812-247-1017.
E-mail addresses: elena.verbitskaya@pop.ioffe.rssi.ru (E. Verbitskaya).

[1] Also at CERN, Geneva, Switzerland.
[2] Also on leave from ITEP, Moscow, Russia.

0168-9002/$ - see front matter
doi:10.1016/j.nima.2003.08.083

Abstract

The recovery of the charge collection efficiency (CCE) at low temperatures, the so-called ''Lazarus effect'', was studied in Si detectors irradiated by fast reactor neutrons, by protons of medium and high energy, by pions and by gamma-rays. The experimental results show that the Lazarus effect is observed: (a) after all types of irradiation; (b) before and after space charge sign inversion; (c) only in detectors that are biased at voltages resulting in partial depletion at room temperature. The experimental temperature dependence of the CCE for proton-irradiated detectors shows non-monotonic behaviour with a maximum at a temperature defined as the CCE recovery temperature. The model of the effect for proton-irradiated detectors agrees well with that developed earlier for detectors irradiated by neutrons. The same midgap acceptor-type and donor-type levels are responsible for the Lazarus effect in detectors irradiated by neutrons and by protons. A new, abnormal ''zigzag''-shaped temperature dependence of the CCE was observed for detectors irradiated by all particles (neutrons, protons and pions) and by an ultra-high dose of γ-rays, when operating at low bias voltages. This effect is explained in the framework of the double-peak electric field distribution model for heavily irradiated detectors. The redistribution of the space charge region depth between the depleted regions adjacent to p^+ and n^+ contacts is responsible for the ''zigzag''- shaped curves. It is shown that the CCE recovery temperature increases with reverse bias in all detectors, regardless of the type of radiation.

PACS: 29.40; 72.20.J; 81.40.X

Keywords: Silicon detectors; Radiation hardness; Charge collection efficiency; Carrier trapping; Electric field distribution

1. Introduction

Silicon detectors are widely used in high-energy physics experiments. The preference for this material, over other semiconductors for the mass production of detectors, is mainly due to two factors:

- the high quality of the initial material, and its availability with suitable well-known parameters (resistivity ρ, wafer dimensions, etc.);
- the availability of mature technology for processing the devices with advanced designs, also including electronic components.

The radiation hardness of silicon, however, leaves much to be desired, since the high quality of the initial bulk material paradoxically renders it vulnerable to radiation damage. This is due to the fact that in high resistivity Si the concentration of radiation-induced defects can easily (at relatively low fluences, e.g. $\geqslant 10^{13}$ n cm^{-2}) exceed the low concentration of effective doping (in the order of 10^{12} cm^{-3}), which alters and controls the detector electrical behaviour. Accumulation of defects in the silicon bulk leads to an increase of the reverse current, and of the full depletion voltage, which may entail incomplete charge collection. Numerous attempts to improve the radiation tolerance of silicon have shown that the introduction of oxygen into the Si bulk is one of the best ways of achieving this goal [1–4]. This procedure enabled a significant reduction in the radiation degradation rate for γ-irradiated detectors [5–7]. However, the improvement in charged hadron beams was by only a factor of 2, whereas for neutron-irradiated detectors a positive effect was observed only in the range of low and medium fluences [2–4,8].

These limitations have stimulated our search for alternative methods of radiation hardening, based on the optimization of the detector in a wider range of operating parameters. One of the most efficient methods is to operate the detector at low temperature. Earlier studies [9–11] have shown that the CCE recovers best at a temperature of 130–140 K and reaches 100% and 50% for neutron fluences F_n of 1×10^{14} and 5×10^{14} cm^{-2}, respectively. A similar effect was also observed in strip detectors irradiated by high-energy protons [12,13]. This effect of CCE recovery at low temperatures has been named the Lazarus effect [9].

We present in this paper experimental results on the CCE recovery for Si p^+–n junction detectors

exposed to different types of radiations: fast neutrons, medium- and high-energy protons, pions and γ-rays. Measurements of the CCE were made as a function of the reverse bias voltage (V) using the Transient Current Technique (TCT), with generation of non-equilibrium carriers by a pulsed laser or ^{90}Sr beta source, in the temperature (T) range of 300–100 K. The experimental data show that the Lazarus effect is observed for all types of irradiation, and only in detectors that are biased at voltages resulting in partial depletion at room temperature. The analysis of the experimental temperature dependence of the CCE is based on the model of the Lazarus effect developed earlier for neutron-irradiated detectors [14]. An attempt is made to develop a more advanced model of the Lazarus effect, considering peculiarities of the electric field distribution $E(x)$, including a double-peak (DP) profile, and of the redistributions of potential and space charge region (SCR) depths in the depleted region of heavily irradiated detectors.

2. Modelling of the CCE recovery for neutron-irradiated detectors

Experimental results on detectors irradiated by neutrons up to fluences in the range 1×10^{14}–1×10^{15} cm^{-2}, are presented in Refs. [10,11], showed that the temperature dependence of the CCE, $\eta(T)$, is non-monotonic. Its maximum $\eta(T_r)$ varies with F_n, whereas the temperature T_r, at which the maximum is reached (the Lazarus effect temperature, or CCE recovery temperature), is practically independent of the fluence and is in the range 130–140 K. Evidently, the non-monotonic $\eta(T)$ originates from the competition between two processes having different temperature dependences. The model developed in Ref. [14] incorporates two related and temperature-dependent phenomena: the reduction with cooling of the bulk generation current and of the charged fractions of the deep levels (DLS). Two mechanisms are considered for the degradation of the collected charge, caused by the radiation damage in the detector:

- charge loss due to trapping of non-equilibrium carriers by deep levels during the charge collection time;
- partial depletion of the detector since the high-resistivity neutral base region acts as a capacitive divider.

The charge collection efficiency associated with carrier trapping $\eta_t(T)$ is based on Hecht's relation, and for short-range particles and MIPs they are defined by Eqs. (1a) and (1b), respectively,

$$\eta_i(T) = \frac{v\tau}{w}\left[1 - \exp\left(-\frac{v\tau}{w}\right)\right], \tag{1a}$$

$$\eta_i(T) = \left\{\frac{v_e\tau_e}{w}\left[1 - \frac{v_e\tau_e}{w}\left(1 - \exp\left(-\frac{v_e\tau_e}{w}\right)\right)\right]\right\} + \left\{\frac{v_h\tau_h}{w}\left[1 - \frac{v_h\tau_h}{w}\left(1 - \exp\left(-\frac{v_h\tau_h}{w}\right)\right)\right]\right\}, \tag{1b}$$

where v is the drift velocity, τ is the trapping time constant, w is the space charge region depth, and the subscripts e and h refer to electrons and holes, respectively.

The trapping time constant is defined as

$$\tau = \frac{1}{\sigma v_{th} N_{tt}}. \tag{2}$$

In Eq. (2) σ is the effective carrier capture cross-section for trapping centres with the total concentration N_{tt}, and v_{th} is the thermal velocity of the carrier. The temperature dependence of $\eta_t(T)$ arises mainly from that of τ, obtained from the parameters in Eq. (2). Power-law dependences are theoretically predicted for σ [15] and v_{th}, resulting in σ increasing with cooling. The concentration of trapping centres N_{tt}, which contribute to $\eta_t(T)$, is the sum of the concentrations of all types of traps: charged deep donors N^+_{DD} and deep acceptors N^-_{DA}, and neutral deep levels N^0_{DL}:

$$N_{tt} = |N^+_{DD}| + |N^-_{DA}| + N^0_{DL}. \tag{3}$$

This may also be temperature dependent and give an even stronger dependence as compared with those for σ and v_{th}, due to the exponential nature of charge state changes with temperature.

The second component of the CCE, labelled $\eta_g(T)$, is related to the partial depletion of a detector, and arises from a geometrical factor F_g, usually defined as the ratio of the SCR depth w to the detector thickness d:

$$F_g = \frac{w}{d}. \tag{4}$$

Note that for MIPs this component is given by

$$\eta_g = \left(\frac{w}{d}\right)^2 = F_g^2, \tag{5}$$

since, of the electron–hole (e–h) pairs created in the thickness d, only the fraction w/d which is generated in the depleted region contributes to the signal. The overall temperature dependence $\eta(T)$ then arises from the dependence of w on T through:

$$w^2 = \frac{2\varepsilon\varepsilon_0 V}{e|N_{\text{eff}}|}, \tag{6}$$

where ε is the relative permittivity of Si, ε_0 is the permittivity of vacuum, e is the elementary charge and N_{eff} is the effective concentration of charged centres in the SCR, defined as the difference between the concentrations of positively charged donors and negatively charged acceptors. These are DLs for heavily irradiated detectors in the entire temperature range with the exception of low T where a contribution from shallow levels ($N_{\text{SL}}^{+/-}$) should be considered:

$$N_{\text{eff}} = |N_{\text{DD}}^{+}| - |N_{\text{DA}}^{-}| + |N_{\text{SL}}^{+/-}|. \tag{7}$$

These concentrations are also temperature dependent and the sign of N_{eff} is determined by the relative contributions of the charges. The total $\eta(T)$ is a product of both trapping and geometrical components:

$$\eta(T) = \eta_t(T)\eta_g(T). \tag{8}$$

The concentration N_{tt} responsible for $\eta_t(T)$ is the sum of the total concentrations of deep donors and acceptors, whereas N_{eff}, which controls $\eta_g(T)$, depends on the difference between the charged fraction concentrations only. In the case of large and close concentrations of deep donors and deep acceptors the sum of the two is much less sensitive to any changes than their difference. Therefore, the trapping component $\eta_t(T)$ is less sensitive than $\eta_g(T)$ to the changes with temperature of the charged DL concentrations.

The fit of Eq. (8) to the experimental $\eta(T)$ for neutron-irradiated detectors is described in detail in Ref. [14]. It has been shown that:

- The main contributor to $\eta(T)$ is the increase of the SCR depth and of the consequent geometrical factor in $\eta(T)$.
- The increase of the SCR depth with decreasing T is caused by the reduction of the charged DL fractions in the SCR.
- The deep midgap energy levels, which are exclusively responsible for the Lazarus effect, are an acceptor-type trap at $E_c - (0.52 \pm 0.01)$ eV and a donor-type trap at $E_v + 0.48$ eV.
- The Lazarus effect can be observed at cryogenic temperatures only in irradiated detectors, which are partially depleted at room temperature (RT) at a given bias voltage.

3. Experimental

Detectors used in this study were processed from n-type standard and oxygen-rich Si. Processing was performed in the Technology Laboratory of Brookhaven National Laboratory (BNL), USA. Different types of radiations were applied in the experiments:

- fast neutrons (1 MeV);
- high-energy protons (24 GeV);
- medium-energy protons (10 MeV),
- pions (190 MeV)
- γ-rays from a ^{60}Co source.

The thicknesses of the samples were 400, 192 and 300 μm for detectors irradiated by neutrons, protons and γ-rays, respectively.

The measurements of charge collection efficiency were performed mainly using the TCT with a laser pulse generation of non-equilibrium carriers, and were carried out in the Ioffe Institute, St. Petersburg, Russia. To minimize the influence of the laser-induced charge on the electric field distribution, the laser light amplitude was kept low enough to reduce the charge down to 10^5 e–h pairs (equivalent to about 4 MIPs). The time resolution was $\sim$1 ns and the temperature range 300–100 K. The measurement procedure is described in Ref. [14]. To prevent accumulation of trapped charge in the detector bulk during the measurements

(detector polarization [16]), the bias voltage was switched off for 30 s before each TCT signal measurement. The collected charge was determined by integrating the current pulse response over the charge collection time. A red laser with a wavelength of 660 nm was used for non-equilibrium carrier generation. Most measurements were performed with laser illumination of the n^+ (back) side of the detector, resulting in $\eta_h(T)$ due to hole collection (holes drifting across the detector thickness). Some samples were also laser illuminated on the p^+ side, yielding $\eta_e(T)$ due to the collection of electrons.

The temperature dependence of the CCE with MIPs was studied at LIP, Portugal, using the cryostat system for absolute CCE measurements described in Ref. [17] and a 3.7×10^6 Bq $^{90}Sr/^{90}Y$ beta source. At each voltage, the CCE was measured immediately after applying bias voltage, before CCE degradation due to polarization. Charge spectra were fitted with Landau distributions, and the peak values (after pedestal subtraction) were normalized to the response of a non-irradiated 400 μm thick detector.

4. Lazarus effect in detectors irradiated by particles (neutrons, protons and pions)

4.1. CCE recovery in neutron-irradiated detectors

Figs. 1a and b show $\eta_{e,h}(V)$, the experimental dependence of the CCE on reverse bias voltage at various temperatures, for the detector # 924-1 that was made of standard Si and was irradiated by neutrons with a fluence $F_n = 5.15 \times 10^{14}$ cm^{-2}. These sets of the curves, determined by laser illumination of the p^+ or n^+ sides for electron or hole collection, respectively, show that at RT, no saturation of the collected charge is observed even at the maximum bias voltage $V = 250$ V. Thus the detector stays partially depleted up to this value. The signal from electrons appears only at $T < 200$ K (Fig. 1a), indicating that the electric field at the p^+ contact is close to zero from RT down to this temperature.

For the analysis the experimental data of $\eta_{e,h}(V,T)$ were re-plotted as a function of T

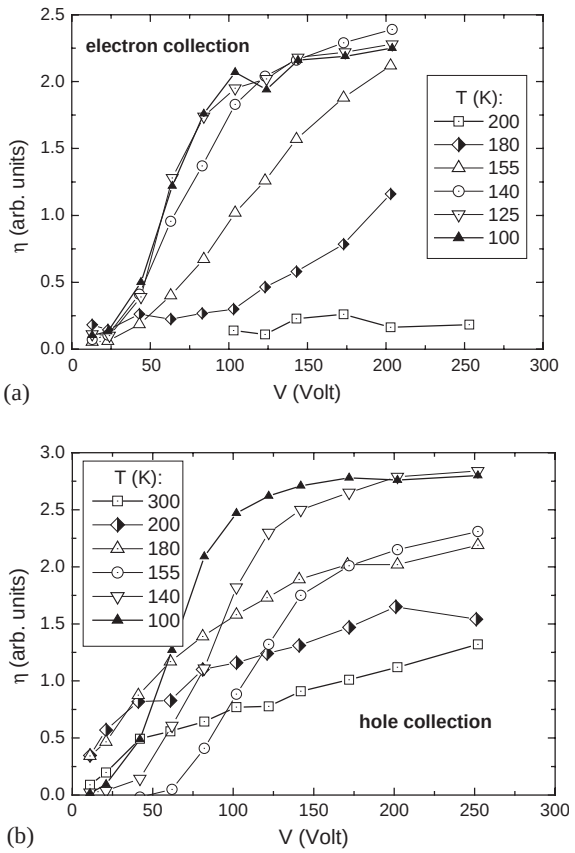

Fig. 1. Experimental dependence of the collected charge on reverse bias voltage at different temperatures for detector # 924-1 made of standard Si and irradiated by $F_n = 5.15 \times 10^{14}$ cm^{-2}, for electron (a), and hole (b) collection.

(Fig. 2a, b). A sharp increase of $\eta_e(T)$ with a reduction in temperature, starting at $T < 200$ K, is observed for electron collection. Meanwhile, for temperatures down to 200 K, $\eta_h(T)$ stays practically constant for hole collection, and increases with V only. After this plateau $\eta_h(T)$ begins to rise. One surprising thing is that at lower bias voltages ($V < 170$ V), $\eta_h(T)$ shows an intermediate maximum at $T = 180$ K and minimum at 155 K. This "zigzag"-shaped feature is less pronounced for electrons and evinced in the narrower range of 170–160 K. The final CCE increase occurs after these irregularities, reaching its maximum in the temperature range of 150–130 K. The same features are detected in $\eta_{e,h}(T)$ for a detector made

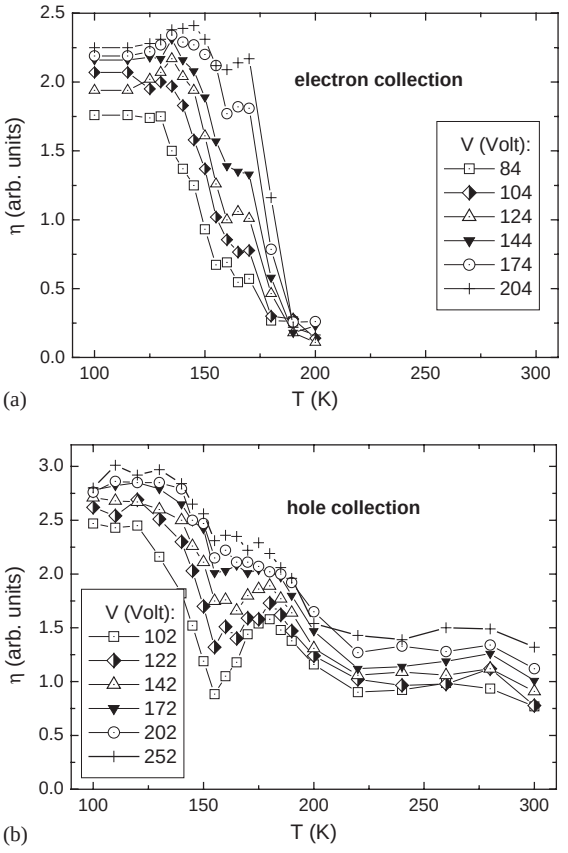

Fig. 2. $\eta(T)$ at different bias voltages for the same detector as in Fig. 1, for electron (a), and hole (b) collection.

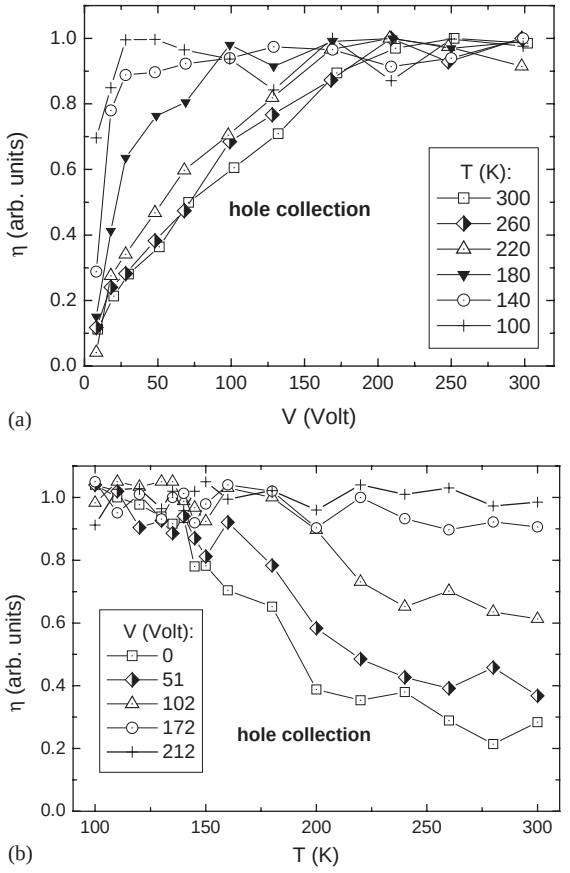

Fig. 3. Experimental $\eta_h(V)$ at various temperatures (a), and $\eta_h(T)$ at different bias voltages (b) for detector # 923-d39 irradiated by high-energy protons at $F_p = 2 \times 10^{14}$ cm^{-2}.

of oxygenated Si and irradiated by the same F_n. This behaviour is different from the earlier dependences reported for MIPs with a single maximum at $T = 130$ to 140 K [10,14]. The analysis of these unusual features will be presented below.

4.2. CCE recovery in detectors irradiated by high-energy protons and pions

The experimental values of $\eta_h(V)$ at various temperatures are shown in Fig. 3a for hole collection for detector # 923-d39 irradiated by high-energy protons to a fluence $F_p = 2 \times 10^{14}$ cm^{-2}. The $\eta_h(V)$ saturation at any $T(\leqslant 300$ K) is evidence of the full depletion of the detector. The bias voltage corresponding to this saturation becomes lower at lower temperatures. Re-plotting the same data as $\eta_h(T)$ (Fig. 3b) shows that near RT the CCE is larger for a higher V. $\eta_h(T)$ then increases monotonically with cooling for any V, and the larger the V the higher the T_r. This recovery agrees with the Lazarus effect model developed for neutron-irradiated detectors, and is caused by the increase of the geometrical factor up to 1 when a detector becomes fully depleted.

We should note that we observed earlier the abnormal "zigzag"-shaped $\eta(T)$ dependence with MIPs for detectors irradiated by protons, and also by pions. These results were obtained in the measurements performed at LIP, Portugal, and

presented at the RD39 collaboration meeting in 2001. The corresponding experimental $\eta(T)$ curves are shown in Fig. 4 for detectors irradiated by protons, with $F_p = 1 \times 10^{15}$ cm^{-2} (the equivalent 1 MeV neutron fluence $F_{neq} = 5 \times 10^{14}$ cm^{-2}), and by a pion fluence $F_\pi = 5 \times 10^{14}$ cm^{-2} ($F_{neq} = 4.5 \times 10^{14}$ cm^{-2}), at two bias voltages: 100 and 200 V. The error bars shown in Fig. 4 include uncertainties from the fit and from the sample thickness.

The remarkable feature is that the temperatures of intermediate extremes in the $\eta(T)$ curves, $\sim$180 and $\sim$160 K for maximum and minimum, respectively, are very close to those in the "zigzag"-shaped dependences for neutron-irradiated detectors (Fig. 2). This suggests that the assembly of DLs responsible for N_{eff} changes with cooling is the same for neutrons and protons.

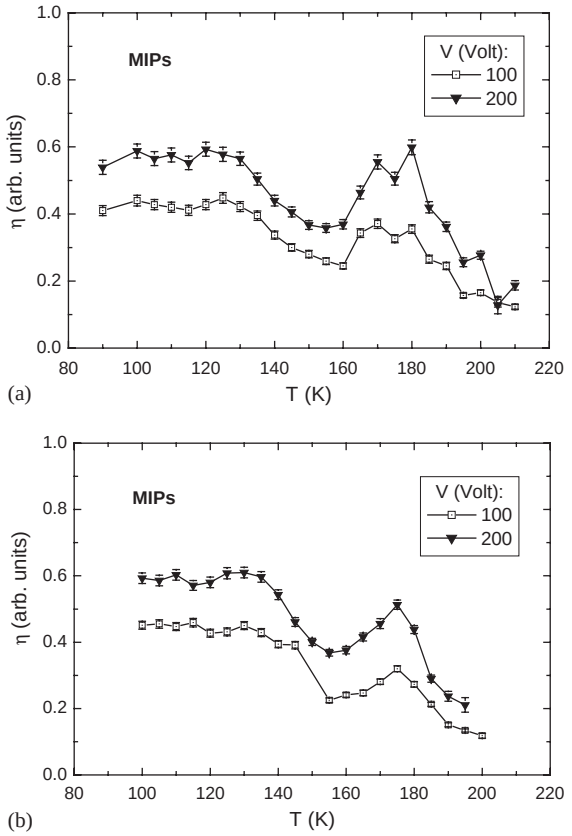

Fig. 4. Experimental $\eta(T)$ dependences for MIP detection for: (a) detector # 1031-2 from standard Si irradiated by 24 GeV protons, $F_p = 1.5 \times 10^{15}$ cm^{-2} ($F_{neq} = 5 \times 10^{14}$ cm^{-2}), and (b) detector # 997-9 from oxygenated Si irradiated by pions, $F_\pi = 5 \times 10^{14}$ cm^{-2} ($F_{neq} = 4.5 \times 10^{14}$ cm^{-2}).

4.3. CCE recovery in detectors irradiated by medium-energy protons before SCSI

In real long-term experiments, the detector experiences all stages of radiation damage, starting from insignificant changes of characteristics up to severe degradation. Earlier investigations of the Lazarus effect dealt with heavily irradiated detectors far beyond space charge sign inversion (SCSI). The question arises whether the CCE recovery at low temperatures can be observed before SCSI. For this, two sets of detectors, made of standard and oxygenated Si, respectively, were irradiated with proton fluences ranging from 2.5×10^{11} to 5×10^{14} cm^{-2}.

The results show that, for both types of detectors, the shapes of $\eta_{e,h}(V)$ and $\eta_{e,h}(T)$ are insensitive to the fluence. They are also quite similar to those observed in samples irradiated by high-energy protons, shown in Fig. 3. In Fig. 5 the current pulse response at $T = 300$ K and different V is presented for detector # 923-5, made of standard Si and irradiated to a fluence $F_p = 1 \times 10^{13}$ cm^{-2}. The flat top of the current pulse

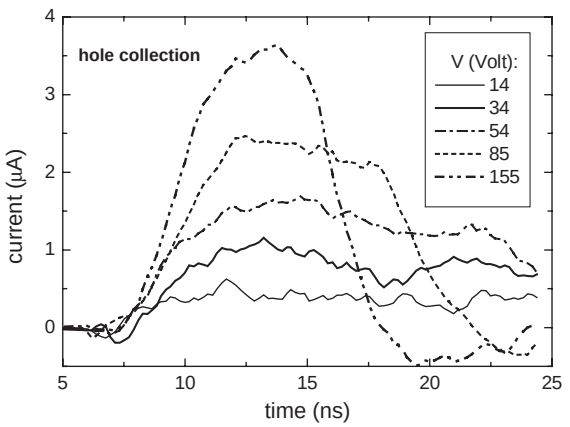

Fig. 5. Transient current response at RT at various bias voltages of detector # 923-5 irradiated by medium-energy protons at $F_p = 1 \times 10^{13}$ cm^{-2}, that is close to the fluence resulting in SCSI.

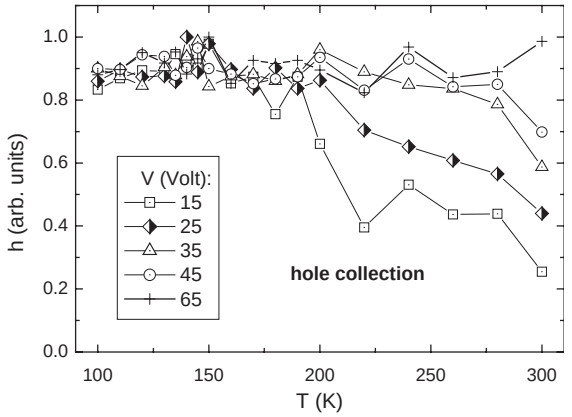

Fig. 6. $\eta_h(T)$ at various bias voltages for the same detector as in Fig. 5.

observed even at low V is evidence of the fact that the detector is close to SCSI, and N_{eff} is negligible compared to the doping concentration in a non-irradiated detector. The $\eta_h(T)$ of Fig. 6 shows the same monotonic CCE recovery with cooling down to T_r as observed for F_p beyond SCSI. Evidently, since the initial N_{eff} at RT is insignificant, the Lazarus effect is detected only at very low V.

5. Observation of the Lazarus effect in detectors irradiated by an ultra-high dose of γ-rays

The investigation of the Lazarus effect in detectors irradiated by γ-rays represents a new step in the study of heavily irradiated Si detectors. The detailed study of detectors irradiated up to the ultra-high dose of 1.76 Grad [6,7] showed that the main difference between characteristics for standard and oxygenated Si is in the evolution of N_{eff} with dose. Negative space charge is introduced in standard Si detectors, resulting in the SCSI that is routinely detected in Si detectors heavily irradiated by other types of radiations. On the contrary, in detectors made of oxygenated Si, positive space charge is accumulated with increasing dose and no SCSI is revealed up to 1.76 Grad. It should also be noted that the rate for the introduction of negative charge in standard Si detectors is one order of magnitude larger than that of positive charge in oxygenated Si detectors [7]. Since the CCE recovery is controlled by the reduction of $|N_{eff}|$ with cooling, one can expect to see differences in the effects in various types of Si.

The experimental values of $\eta_h(T)$ at various bias voltages in the interval 50–400 V are shown in Fig. 7, for the detector made of standard Si and irradiated to a dose of 1.65 Grad. Note that at RT N_{eff} is negative, which is usual for detectors heavily irradiated by other particles. In the temperature range 300–220 K $\eta_h(T)$ is nearly constant and increases only with reverse voltage. It then increases steeply at $T \approx 220$ K when the temperature is reduced. At lower bias voltages of 50 and 80 V, however, there is a drastic drop of the signal practically down to zero at $T = 200$ K, after which the signal grows sharply. The surprising thing is that this peculiarity is accompanied by the inversion of the sign of N_{eff} from negative to positive upon cooling, as can be seen in the current pulse response in the temperature range 200–150 K. With further cooling down to 100 K, the CCE is nearly constant while space charge stays positive. For the analysis of the temperature dependence of N_{eff}, the values of N_{eff} were derived from the full depletion voltage V_{Qsat} corresponding to the CCE saturation in the curves of $\eta_h(V)$ at different temperatures. The temperature dependence of N_{eff} for a detector made of standard Si shows non-monotonic behaviour with SCSI (Fig. 8), which is quite unique for irradiated

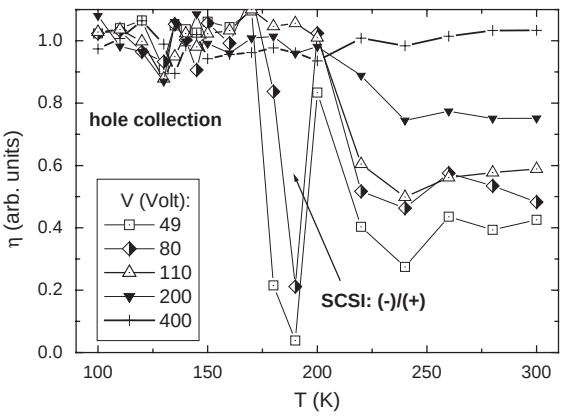

Fig. 7. Efficiency for hole collection, $\eta_h(T)$, at various bias voltages for a detector made of standard Si irradiated by ^{60}Co γ-rays to a dose of 1.65 Grad.

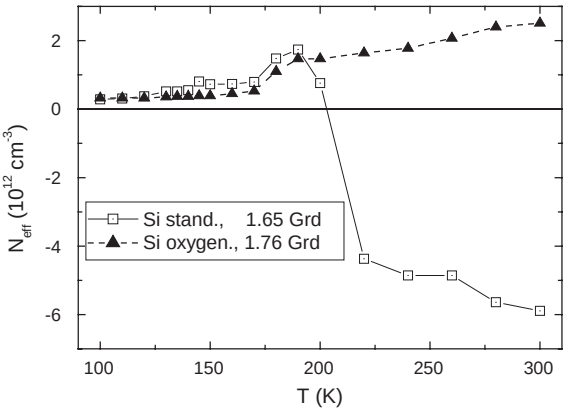

Fig. 8. $N_{\rm eff}(T)$ for detectors made of standard and oxygenated Si and irradiated by an ultra-high dose of γ-rays.

detectors. The slight increase in $N_{\rm eff}$ from its initial value of -6×10^{12} cm^{-3}, which occurs from RT to 220 K, is followed by its sharp increase up to about zero and SCSI at $T=200$ K. The maximum positive $N_{\rm eff}$ of 2×10^{12} cm^{-3} is achieved at $T\approx190$ K after which $N_{\rm eff}$ goes down monotonically to a saturated value of $\sim3\times10^{11}$ cm^{-3}. Note that at $V>100$ V, $\eta_{\rm h}(T)$ curves show standard behaviour, with the CCE only reaching its maximum at $T_{\rm r}$ (Fig. 7).

In contrast with standard detectors, the experimental $\eta_{\rm h}(T)$ for oxygenated detectors irradiated by γ-rays shows normal behaviour. At lower bias voltages, ranging from 21–71 V, $\eta_{\rm h}(T)$ is nearly constant in the temperature interval 300 to 200 K and increases only slightly with reverse voltage. Then $\eta_{\rm h}(T)$ increases steeply at $T\approx180$–200 K when the temperature is reduced, reaching its maximum at T ranging from 150 to 180 K. At higher bias voltages ($V\geqslant100$ V) the CCE recovery is more gradual; $T_{\rm r}$ is higher than 200 K and depends on V. The analysis of the current pulse response shows that the space charge stays positive from RT down to 100 K. The temperature dependence of $N_{\rm eff}$ was determined by the same procedure as was used for detectors made of standard Si, and is presented in Fig. 8 along with the data for the standard Si detector. It is important to note that at $T<190$ K $N_{\rm eff}$ has the same positive value in both types of silicon detectors.

6. Lazarus effect modelling for detectors irradiated by protons

In the model of the Lazarus effect developed earlier for neutron-irradiated detectors [10,14], two main features emerged:

- only the midgap energy levels, in particular the deep acceptor with an energy of $E_{\rm c}-0.52$ eV, are responsible for the reduction of $N_{\rm eff}$, and for the corresponding recovery of the CCE;
- the assumption of the mean electric field in the SCR, defined as $\langle E\rangle=V/w$, proved reasonable for the modelling of the experimental $\eta_{\rm MIP}(T)$.

Hence for modelling the $\eta_{\rm h,e}(T)$ for detectors irradiated by different types of radiations, a knowledge of microscopic defect spectra is initially required to answer the question of whether the same midgap energy levels are introduced by the other types of radiations. Fig. 9 shows the I-DLTS spectrum of detector # 923-d39 from standard Si irradiated by 24 GeV protons with a fluence of 2×10^{14} cm^{-2}. The fit of the experimental curve with multiple overlapping peaks reveals two midgap energy levels:

- deep donor (DD) with the activation energy $E_{\rm a}=E_{\rm v}+0.48$ eV,
- deep acceptor (DA) with $E_{\rm a}=E_{\rm c}-0.515$ eV

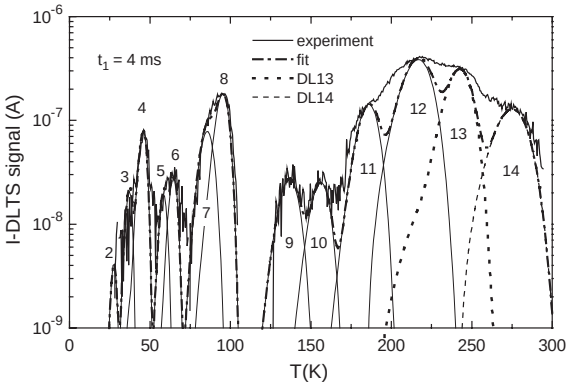

Fig. 9. Experimental and fitted I-DLTS spectrum for detector # 923-d39 made of standard Si and irradiated by high-energy protons. $E_{\rm p}=24$ GeV, $F_{\rm p}=2\times10^{14}$ cm^{-2}. Peaks ## 13 and 14 are due to a deep donor at $E_{\rm v}+0.48$ eV and a deep acceptor at $E_{\rm c}-0.515$ eV, respectively.

(peaks # 13 and 14, respectively, in Fig. 9). The same result was also obtained for detectors irradiated by medium-energy protons. These data agree with our earlier measurements of microscopic defect spectra that showed the similarity of defect assembly in Si detectors irradiated by neutrons and by 24 GeV protons [18]. Hence the midgap deep levels induced by protons are similar to those introduced by neutrons and can be tested for fitting of the $\eta_h(T)$.

The experimental data fitting procedure, using the model developed for neutron-irradiated detectors, is described in detail in Ref. [14], and was briefly presented in Section 2. Note that in Ref. [14] we used Eq. (1b), which is valid for $\eta_{MIP}(T)$, while in the present study Eq. (1a) was applied, with parameters specific for hole collection, since non-equilibrium carriers were generated near the n^+ contact. The result of the CCE recovery fit for the proton-irradiated, standard Si detector # 923-d39 operated at $V = 102$ V is shown in Fig. 10a. This detector was chosen as an example for the detailed study of the Lazarus effect since at the maximum reverse voltage of 300 V used in the TCT measurements, the detector was fully depleted even at RT. This enabled us to compare over a wide temperature range the results obtained using the different approaches described below in Section 7.1. Since $V_{fd} = 210$ V at RT, the detector is only partially depleted at $V = 102$ V. The CCE recovery is gradual and its maximum is reached at $T_r = 180$ K. Parameters of DLs responsible for the Lazarus effect (E_a, σ and total concentrations N_{DD}, N_{DA}) and of the trapping centres (N_{tt} with the assumption that the effective capture cross-section σ is 10^{-15} cm^2) were deduced from the fit. These parameters, along with the effective parameters for reverse current from Ref. [19], which were used for the fit (activation energy, capture cross-section and concentration of generation centres) are compared in Table 1 with the corresponding parameters from the earlier results of Ref. [14] on detectors irradiated by a neutron fluence of 1×10^{14} cm^{-2}. Note that the label "N" used in Table 1 is a common one for all concentrations presented in the table. The effective parameters for reverse current of Si detectors irradiated by different radiations were determined in Ref. [19] from the reverse current dependence on temperature

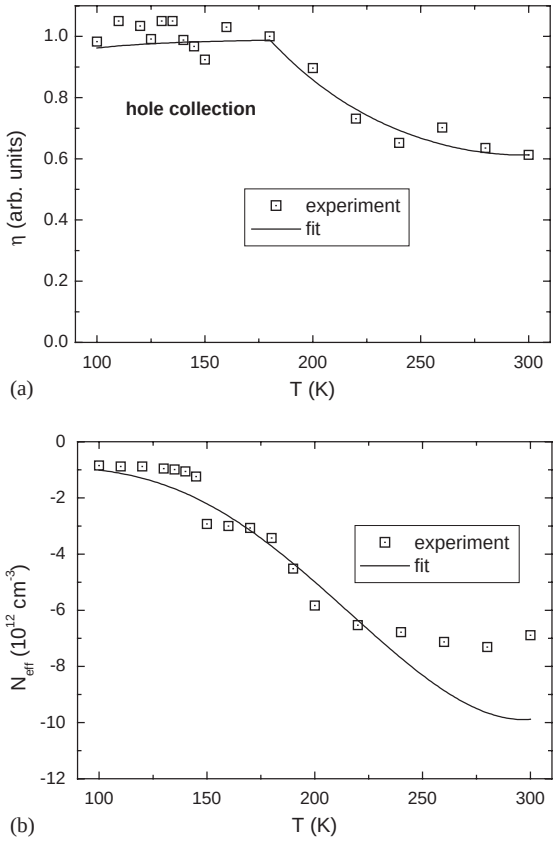

Fig. 10. Experimental and fitted $\eta_h(T)$ (a) and $N_{eff}(T)$ (b) dependences for detector # 923-d39 operated at $V = 102$ V.

according to Shockley–Read–Hall statistics using the model of a single (effective) generation level. The experimental temperature dependence of N_{eff} shown in Fig. 10b (curve "experiment") uses N_{eff} values derived from V_{Qsat}, corresponding to CCE saturation as described in Section 5. It follows from a comparison of the DD and DA concentrations ($\sim 10^{14}$ cm^{-3}) and N_{eff} ($< 10^{13}$ cm^{-3}) that only an insignificant fraction of the DLs contributes to the space charge, as was shown earlier for neutron-irradiated detectors [14]. Meanwhile, the similar values found for N_{DD}, N_{DA} and N_{tt} imply that the neutral states of the midgap defects are responsible for the carrier trapping. The same curve-fitting procedure for $\eta_h(T)$ was also performed for detectors from standard Si irradiated by medium-energy protons. A good fit of the experimental dependence may also be obtained using the same

Table 1
Parameters of deep levels and trapping centres derived from the fitting of CCE on T dependences for detectors irradiated by neutrons and protons

	DD	DA	Trapping centres	Generation current [19]	T_r (K)
Neutrons [14]; $F = 1 \times 10^{14}$ *cm*$^{-2}$; $V = 100$ *V*					132
E_a (eV)	$E_v + 0.48$	$E_c - 0.527$		0.65	
σ (cm^2)	1×10^{-15}	1×10^{-15}	1×10^{-15}	1×10^{-14}	
N(cm^{-3})	2.0×10^{14}	8.0×10^{14}	4.0×10^{14}	2.6×10^{15}	
# *924-d39*; 24 *GeV protons*; $F = 2 \times 10^{14}$ *cm*$^{-2}$; $V = 102$ *V*					180
E_a (eV)	$E_v + 0.48$	$E_c - 0.53$		0.657	
σ (cm^2)	1.2×10^{-15}	1.2×10^{-15}	1×10^{-15}	1×10^{-14}	
N (cm^{-3})	5.8×10^{14}	$5.9.0 \times 10^{14}$	2×10^{14}	6.2×10^{15}	
# *923-5*; 10 *MeV protons*; $F = 5 \times 10^{13}$ *cm*$^{-2}$; $V = 85$ *V*					196
E_a (eV)	$E_v + 0.48$	$E_c - 0.522$		0.657	
σ (cm^2)	2×10^{-15}	1.7×10^{-15}	1×10^{-15}	1×10^{-14}	
N (cm^{-3})	7.8×10^{14}	$2.35.0 \times 10^{14}$	4.5×10^{14}	6.2×10^{15}	

two midgap energy levels. The parameters derived from the fit are presented in Table 1 for the standard Si detector # 923-5 irradiated by a fluence of 5×10^{13} cm^{-2} and operating at $V = 85$ V.

Hence it is shown that the DLs responsible for the CCE recovery are identical for detectors irradiated by neutrons and protons. With the assumption of the mean E in the SCR, the temperature dependences of the electric field and the total η_h are plotted in Fig. 11 for detector # 923-d39 irradiated by high-energy protons, for different bias voltages in the range 51–212 V. The calculated curves $\eta_h(T)$ agree nicely with the experimental data (Fig. 3b). The electric field is proportional to V and decreases with T while the detector stays partially depleted ($\eta_g < 1$), and becomes constant for $T < T_r$.

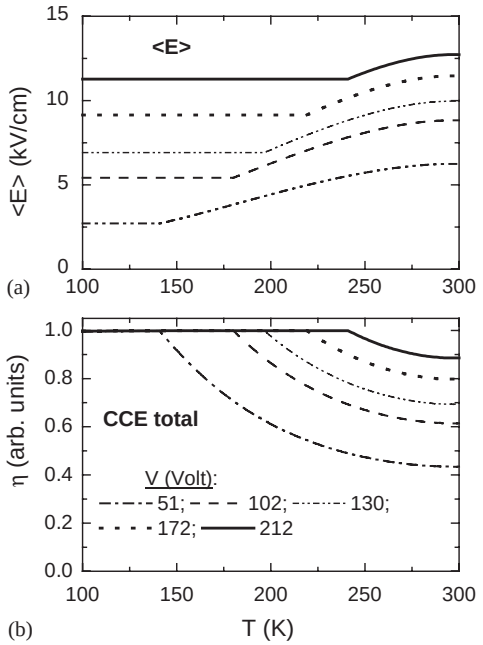

Fig. 11. Calculated temperature dependence of the mean electric field (a) and $\eta_h(T)$ (b) for the same detector as in Fig. 9, assuming a constant mean electric field in the SCR.

7. Advanced model of the Lazarus effect considering electric field distribution in heavily irradiated detectors

7.1. Lazarus effect with a consideration of double peak electric field distribution controlled by carrier trapping

We should emphasize that the constant electric field in the SCR, assumed in the analysis, and even a linear, single peak (SP) distribution of electric field $E(x)$ with a maximum at one of the contacts, are rather unrealistic in heavily irradiated detectors. Due to the trapping of free carriers from the bulk generation current, the electric field has a DP profile with two maxima near the detector contacts

[20]. This effect is usually observed in detectors irradiated beyond SCSI. At lower bias voltages SCRs exist near each of the contacts. With increasing bias voltage, the SCR expands from the n^+ contact, and then a pinch-off occurs at $V_{p\text{-off}}$. At some V (actually V_{Qsat}) a linear distribution of $E(x)$ with a single peak is achieved in the entire detector structure. The DP $E(x)$ profile is observable as a DP pulse shape in the current pulse response, which transforms into a pulse with a single slope top with increasing bias. Starting from V_{Qsat} corresponding to a fully depleted detector and saturation of $\eta_h(V)$, Eq. (6) describes adequately the relationship between N_{eff} and V. The reverse bias V_{Qsat} at each T may be used for determining N_{eff} and its temperature dependence. It has been shown in Ref. [20] that the two midgap energy levels are responsible for the DP electric field, which are the same as those used in our study for the $\eta_h(T)$ fit.

In the experimental $N_{eff}(T)$ curve for the proton-irradiated detector # 923-d39 (Fig. 10b), the N_{eff} determined according to the above procedure, has a value of -7×10^{12} cm^{-3} at RT. The entire curve shows a monotonic increase of N_{eff} (reduction of the negative charge) in the range 220–145 K, while in the temperature intervals above and below this region the changes of N_{eff} are quite insignificant. Using the $\langle E \rangle$ approach, simultaneous fits of both $\eta_h(T)$ and $N_{eff}(T)$, shown in Figs. 10a and b, respectively, may be obtained with the same parameters of midgap defect levels as those listed in Table 1, which were deduced from $\eta_h(T)$ alone. The fit of $N_{eff}(T)$ shows a good agreement with the experimental data in the wide temperature range from 250 to 100 K (Fig. 10b).

Evidently, trapping entails not only the temperature dependence of $N_{eff}(T)$ but also the non-uniform distribution $N_{eff}(x)$ of the space charge. Consideration of this distribution is important for adequate modelling of the Lazarus effect. As can be seen from the experimental $\eta_h(T)$ curve (Fig. 10a) and simulations of $\langle E \rangle(T)$ and $\eta_h(T)$ presented in Fig. 11, at $V = 102$ V the detector becomes fully depleted and the CCE reaches its maximum at $T_r = 180$ K. Simulation of the $E(x)$ and $N_{eff}(x)$ (Figs. 12a and b, respectively) including the trapping effect as described in Ref. [20] and

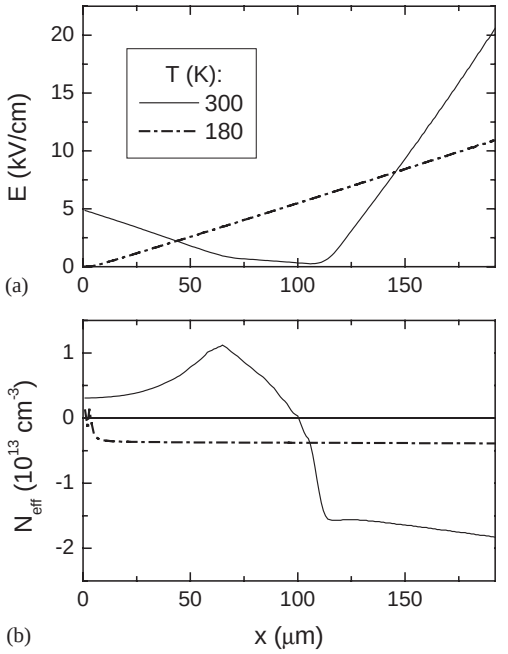

Fig. 12. Simulations of the distributions $E(x)$ (a) and $N_{eff}(x)$ (b) for detector # 923-d39 operated at $V = 102$ V. The simulation takes into account the electric field distribution controlled by carrier trapping.

the deep level parameters deduced from $\eta(T)$ (Table 1), and comparison with the results obtained without trapping (Fig. 10a), show the following characteristics at $V = 102$ V:

- At $T = 300$ K a DP electric field profile is distributed over the entire detector thickness ($\sim$200 μm). This profile is asymmetric with a maximum at the n^+ contact. Accordingly, the regions of positive and negative N_{eff} expand from the p^+ and n^+ contacts, respectively.
- At $T = T_r = 180$ K the detector is practically fully depleted, in agreement with the result deduced from the fit of $\eta_h(T)$ considering $\langle E \rangle$ only, and $E(x)$ becomes linear. Then $N_{eff} = -3.9 \times 10^{12}$ cm^{-3} at the n^+ contact, and is practically constant in the entire SCR.
- At $T = T_r$, $\langle E \rangle = \overline{E(x)} \approx 5.5$ kV/cm (where $\overline{E(x)}$ is the mean electric field determined from the profile of $E(x)$ at 180 K presented in Fig. 12a);
- Comparison of the numerical data gave the following relationship between space charge

concentrations at $T = T_r$ determined from different approaches:

- $N_{eff} = -3.4 \times 10^{12}$ cm^{-3} is derived from the fit of $\eta_h(T)$ using $\langle E \rangle$ approximation only;
- $N_{eff} = -3.5 \times 10^{12}$ cm^{-3} is extracted from the potential dependences $\eta_h(V)$;
- $N_{eff} = -3.9 \times 10^{12}$ cm^{-3} is calculated from the distributions $E(x)$ and $N_{eff}(x)$, controlled by carrier trapping from bulk generation current.

Thus, at T_r, nice agreement (within 15%) is obtained for the values of two main characteristics of the irradiated detector—the electric field and space charge density. Differences are within the experimental error, thus the three approaches give the same result. This fact leads us to conclude that if the current pulse response and $\eta_h(T)$ do not show any abnormal features, the assumption of the mean electric field $\langle E \rangle$ yields correct results for the fit of $\eta_h(T)$, for the temperature of the CCE recovery, and for N_{eff}.

Finally we would emphasize that the dependence of T_r on reverse voltage, for all detectors of the present study, was ascending and close to linear. This dependence is shown in Fig. 13 for the proton-irradiated detector #923-d39. The increase of T_r with V is due to the fact that the higher the V, the larger the w at RT, and the smaller the reduction of N_{eff} needed for a detector to reach full depletion (i.e. the temperature can be higher).

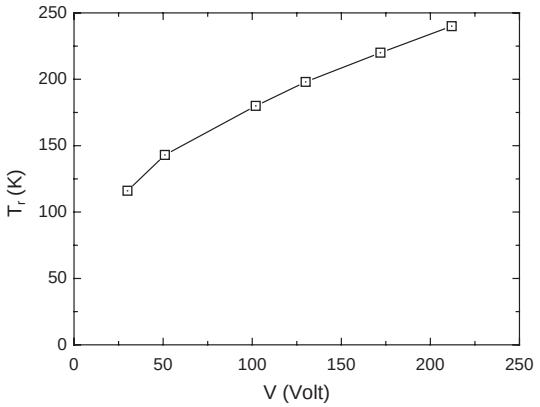

Fig. 13. Dependence of T_r on reverse bias voltage for detector # 923-d39.

7.2. "Zigzag"-shaped Lazarus effect: CCE recovery controlled by redistribution of SCR depth

It was shown in Sections 4 and 5 that for detectors heavily irradiated by strongly interacting particles (n, p, π) and γ-rays and operated at lower V, $\eta_h(T)$ is non-monotonic and reveals an abnormal, abrupt drop of the CCE followed by sharp recovery upon further cooling. This "zigzag"-shaped $\eta_h(T)$ dependence can be explained considering the DP $E(x)$ controlled by carrier trapping, as described above in Section 7.1 for the case of proton-irradiated detectors, accompanied by the redistribution of the potential, electric field and SCR depth within the thickness of the detector. For an explanation of these effects, $\eta_e(T)$ and $\eta_h(T)$ are compared in Fig. 14 for detector # 924-1, made of standard Si irradiated by a neutron fluence of 5.15×10^{14} cm^{-2} and operated at $V =$ 102 V. In the temperature range from 300 to 200 K, only $\eta_h(T)$ is non-zero. This implies that at lower V the SCR expands only from the n^+ contact. Meanwhile, the $\eta_e(T)$ deviates from zero only below 200 K. In the range from 200 to 180 K, both $\eta_e(T)$ and $\eta_h(T)$ rise, suggesting an increase of the SCR depths adjacent to the p^+ and n^+ contacts, w_p and w_n, respectively. Redistributions of the electric field and the space charge regions inside the detector structure with T decreasing from 200 to 180 K are shown schematically in Fig. 15 (solid and dashed lines, respectively). Then, in the interval from 180 to 155 K an abrupt drop of $\eta_h(T)$ is observed, whereas $\eta_e(T)$ increases. A reasonable explanation of this effect may be associated with the redistribution of the space charge region depth between the SCRs at both contacts, namely the increase of w_p and the reduction of w_n (Fig. 15, dotted line). This redistribution may be caused by the changes in sharing of applied bias voltage between w_n and w_p, or changes of N_{eff} with temperature in these regions. Since below $T = 155$ K a further increase of both $\eta_e(T)$ and $\eta_h(T)$ occurs, it is clear that at $T = 155$ K there is an electrically neutral base (ENB) gap region between the two space charge regions adjacent to the p^+ and n^+ contacts. This

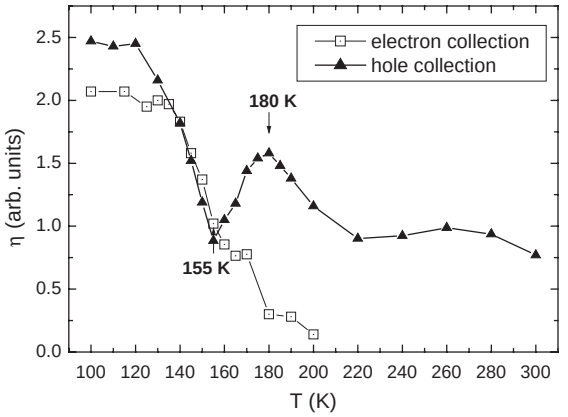

Fig. 14. $\eta_e(T)$ and $\eta_h(T)$ for detector # 924-1 made of standard Si, irradiated by neutron fluence of 5.15×10^{14} cm^{-2} and operated at $V = 102$ V.

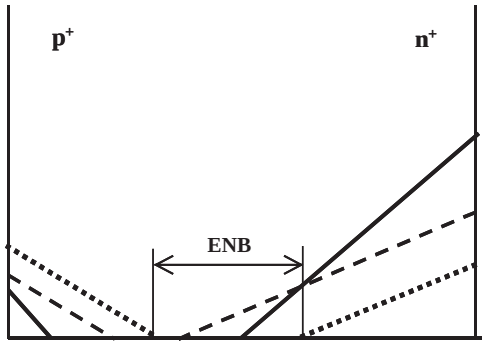

Fig. 15. Redistribution of the electric field profile and SCR depths with temperature reduction: from 200 K (solid lines) down to 180 K (dashed lines) and to 155 K (dotted lines) for the same detector as in Fig. 14.

gap vanishes in the range of 130–120 K, i.e. a pinch-off occurs and the maximum is achieved for both $\eta_e(T)$ and $\eta_h(T)$.

Note that the "zigzag"-shaped $\eta(T)$ was also observed for: (a) detectors from oxygenated Si irradiated by the same neutron fluence as that for standard detectors, (b) detectors from standard Si irradiated by an ultra-high γ-ray dose, and (c) detectors from standard and oxygenated Si irradiated by high-energy protons and pions. This effect was insensitive to the method of non-equilibrium carrier generation: using red laser (a and b), or MIPs (c). For detectors irradiated by γ-rays the drastic changes of $\eta_h(T)$, (a drop down to zero at T in the vicinity of 200 K, and subsequent abrupt increase), are more pronounced than in detectors irradiated by particles and are accompanied by changes of the sign of N_{eff}. This difference arises most likely from the different Si recoil spectra and therefore initial defect introduction. Evidently, adequate modelling of "zigzag"-shaped features needs further study, considering the redistributions of $E(x)$ and SCR depths between the contacts. Thus the precise determination of the numerical parameters of charge collection cannot be performed using the simplified model employing the mean electric field.

8. Conclusions

1. Experimental study of the CCE recovery at cryogenic temperatures in detectors irradiated by neutrons, medium- and high-energy protons, pions and γ-rays have shown that the Lazarus effect is observed:

- with all types of irradiation;
- irrespective of the space charge sign at RT;
- only in detectors that are biased at voltages resulting in partial depletion at RT.

2. The non-monotonic $\eta_h(T)$, with a maximum at T_r, arises from the competition between two temperature-dependent processes controlling the charge losses: the reduction of the space charge concentration in the depleted region dominating above T_r, and the enhancement of charge carrier trapping that prevails below T_r.

3. When decreasing the temperature of detectors irradiated beyond SCSI, the linear electric field expands from the n^+-contact inside the detector bulk (SP $E(x)$). The maximum of $\eta(T)$ is achieved when the detector becomes fully depleted. The recovery of CCE results directly from the collection of charge carriers exclusively via a fast drift process.

4. An abnormal "zigzag"-shaped $\eta(T)$ is revealed in detectors irradiated by strongly interacting particles (neutrons, protons and pions) while operated at voltages below pinch-off voltage. This effect is related to the DP electric field distribution

in heavily irradiated detectors and to the redistribution of the space charge region depth between the depleted regions adjacent to the p^+ and n^+ contacts.

5. The Lazarus effect in detectors irradiated by an ultra-high dose of γ-rays is observed for both signs of the space charge that depends on the bulk material (negative for standard Si and positive for oxygenated Si). In detectors made of standard Si, where SCSI occurs, the abnormal "zigzag"-shaped $\eta(T)$ is observed at lower V. This effect is similar to that evinced in detectors irradiated by particles.

6. The recovery temperature T_r of the Lazarus effect increases with reverse bias.

7. The same midgap acceptor-type and donor-type levels are responsible for the Lazarus effect in detectors irradiated by neutrons and protons. The relationship between the CCE recovery and defect assembly induced by γ-rays needs further study.

References

[1] Z. Li, et al., IEEE Trans. Nucl. Sci. NS- 42 (4) (1995) 219.
[2] G. Lindström, et al., Nucl. Instr. and Meth. A 465 (2001) 60.
[3] G. Lindström, et al., Nucl. Instr. and Meth. A 466 (2001) 308.
[4] RD48 Status Report, CERN-LHCC-2000-009, 1999.
[5] B. Dezillie, et al., IEEE Trans. Nucl. Sci. NS-47 (2001) 1892.
[6] E. Fretwurst, G. Lindström, J. Stahl, I. Pintillie, Z. Li, J. Kierstead, E. Verbitskaya, R. Röder, Nucl. Instr. and Meth. (2003) these Proceedings.
[7] Z. Li, E. Verbitskaya, E. Fretwurst, J. Kierstead, V. Eremin, I. Ilyashenko, R. Röder, C. Wilburn, Nucl. Instr. and Meth. (2003) these Proceedings.
[8] Z. Li, et al., Nucl. Instr. and Meth. A 476 (2002) 628.
[9] V. Palmieri, K. Borer, S. Janos, C. Da Via, L. Casagrande, Nucl. Instr. and Meth. A 413 (1998) 475.
[10] K. Borer, et al., Nucl. Instr. and Meth. A 440 (2000) 5.
[11] T. O. Niinikoski, et al., Nucl. Instr. and Meth. A 476 (2002) 569.
[12] K. Borer, et al., Nucl. Instr. and Meth. A 440 (2000) 17.
[13] L. Casagrande, et al., IEEE Trans. Nucl. Sci. NS-46 (1999) 228.
[14] V. Eremin, V. Eremin, E. Verbitskaya, I. Ilyashenkj, Z. Li, T.O. Niinikoski, G. Ruggiero, Temperature dependence of charge collection efficiency in heavily irradiated silicon detectors: the Lazarus effect model, RD 39 Status Report, CERN-LHCC 2002–004 (2002).
[15] V. N. Abakumov, et al., Sov. Phys. Semicond. 12 (1978) 1.
[16] B. Dezillie, V. Eremin, Z. Li, E. Verbitskaya, Nucl. Instr. and Meth. A 452 (2000) 440.
[17] Z. Li, et al., IEEE Trans. Nucl. Sci. 49 (2002) 1040.
[18] V. Eremin, A. Ivanov, E. Verbitskaya, Z. Li, S.U. Pandey, Nucl. Instr. and Meth. A 426 (1999) 120.
[19] E. Verbitskaya, V. Eremin, I. Ilyashenko, Z. Li, B. Dezillie, Competition of generation channels in reverse current of silicon irradiated detectors, CERN/LEB 2000-005, 5th ROSE Workshop, RD48, March 2000, pp. 300–312.
[20] V. Eremin, E. Verbitskaya, Z. Li, Nucl. Instr. and Meth. A 476 (2002) 556.